Annihilation of vortex dipoles in an Oblate Bose-Einstein Condensate

Shashi Prabhakar, R. P. Singh, S. Gautam, and D. Angom
Theoretical Physics Division, Physical Research Laboratory, Navrangpura, Ahmedabad. 380009. India

We theoretically explore the annihilation of vortex dipoles, generated when an obstacle moves through an oblate Bose-Einstein condensate, and the possible reasons for the annihilation. We show that the grey soliton, which results from the vortex dipole annihilation, is lower in energy than the vortex dipole. We also investigate the annihilation events numerically and observe that the annihilation occurs only when the vortex dipole overtakes the obstacle. Furthermore, we find that the noise reduces the probability of annihilation events. This may explain the lack of annihilation events in experimental realizations.

PACS numbers: 03.75.Mn, 03.75.Kk

I. INTRODUCTION

One of the important developments in recent experiments on atomic Bose-Einstein condensates (BECs) is the creation of vortices and the study of their dynamics [1, 2]. Equally important is the very recent experimental observation of a vortex dipole, which consists of a vortex-antivortex pair, when an obstacle moves through a BEC [3] and *in situ* observation of vortex dipoles produced through phase imprinting [4]. In superfluids, the vortices carry quantized angular momenta and are the topological defects, which often serve as the conclusive evidence of superfluidity. In a vortex dipole, vortices of opposite charges cancel each other's angular momentum and thus carry only linear momentum. This is the cause of several exotic phenomena like leap frogging, snake instability [5], orbital motion [6], trapping [7], and others. The effects of vortices are widespread in classical fluid flow [8] and optical manipulation [9]. A good description of vortices in superfluids is given in Ref. [10] and review articles [11, 12]. More detailed discussion of vortices is given in Ref. [13].

Among the important phenomena associated with the Bose-Einstein condensate (BEC), the creation, dynamics, and annihilation of vortex dipoles carry lots of information associated with the system. Several methods have been suggested to nucleate vortices. Recently, nucleation of the vortices have been observed experimentally by passing a Gaussian obstacle through the BEC with a speed greater than some critical speed [3]. The trajectories of these vortex dipoles are ring-structured as described in Refs. [14, 15]. Annihilation of vortices in the BEC has been speculated in a number of studies. However, no extensive study has been done so far. Moreover, it has not been observed in the experiments done with an oblate BEC. The study of vortex dipole annihilation will shed light on the process that leads to minimum separation between vortex-antivortex and conditions for annihilation along with other phenomena arising due to dynamics of vortex dipoles.

In this article, we present analytical and numerical results related to vortex dipole annihilation for an oblate BEC at zero temperature. The results have been obtained using Gross-Pitaevskii (GP) equation. In the Section. II of the paper, we provide a brief description of the two-dimensional (2D) GP equation and vortex dipole solutions. Approximate analytic solutions of 2D GP equation with a vortex dipole or a grey soliton, expressed as linear combinations of the eigenstates of trapping potential, are given in Section III. Stability of the solutions are analysed from the energies of the solutions. The numerical results, confirming the analytic results, are discussed in Section IV, and we then conclude.

II. SUPERFLUID VORTEX DIPOLE

In the mean-field approximation, the dynamics of the dilute BEC is very well described by the GP equation

$$i\hbar\partial_t\Psi(\mathbf{r},t) = [\mathcal{H} + U|\Psi(\mathbf{r},t)|^2]\Psi(\mathbf{r},t), \quad (1)$$

where Ψ, $\mathcal{H}$, and U are normalized wave function of the condensate, single-particle Hamiltonian and interaction strength respectively. The complete single-particle Hamiltonian $\mathcal{H}$ consists of a kinetic-energy operator, an axis-symmetric harmonic trapping potential, and a Gaussian obstacle potential, i.e.,

$$\mathcal{H} = -\frac{\hbar^2}{2m}\nabla^2 + \frac{m\omega^2}{2}(x^2+\alpha^2y^2+\beta^2z^2) + V_{\rm obs}(x,y,t), \quad (2)$$

where α and β are the anisotropies along y and z axis respectively, and $V_{\rm obs}(x,y,t)$ is the repulsive Gaussian obstacle potential. Experimentally, obstacle potential is produced by a laser beam which is blue-detuned with respect to the frequency of the atomic transition and can be written as

$$V_{\rm obs}(x,y,t) = V_0(t)\exp\left[-2\frac{(x-vt)^2+y^2}{w_0^2}\right], \quad (3)$$

where $V_0(t)$ is the potential at the center of the Gaussian obstacle at time t, v is the velocity of the obstacle along x-axis, and w_0 is the width of the obstacle potential. In the present work, we consider the motion of obstacle

along x-axis only. Defining the oscillator length of the trapping potential $a_{\rm osc} = \sqrt{\hbar/(m\omega)}$, and considering $\hbar\omega$ as the unit of energy, we can then rewrite the equations in dimensionless form with transformations $\tilde{\mathbf{r}} = \mathbf{r}/a_{\rm osc}$, $\tilde{t} = t\omega$, and the transformed order parameter

$$\phi(\tilde{\mathbf{r}}, \tilde{t}) = \sqrt{\frac{a_{\rm osc}^3}{N}}\Psi(\mathbf{r}, t), \tag{4}$$

where N is the number of atoms in the condensate. For the sake of notational simplicity, hereafter we denote the scaled quantities without tilde in the rest of the manuscript. In the pancake-shaped traps ($\alpha = 1$ and $\beta \gg 1$), the order parameter

$$\phi(\mathbf{r}, t) = \psi(x, y, t)\zeta(t)\exp(-i\beta t/2), \tag{5}$$

where $\zeta = (\beta/(2\pi))^{1/4}\exp(-\beta z^2/4)$ is the order parameter in the axial direction. The Eq. (1) can then be reduced to the two dimensional form

$$\left[-\frac{1}{2}\left(\frac{\partial^2}{\partial x^2} + \frac{\partial^2}{\partial y^2}\right) + \frac{x^2 + y^2}{2} + V_{\rm obs}(x, y, t) + u|\psi(\mathbf{r}, t)|^2 - i\frac{\partial}{\partial t}\right]\psi(\mathbf{r}, t) = 0, \tag{6}$$

here $u = 2aN\sqrt{2\pi\beta}/a_{\rm osc}$, where a is the s-wave scattering length, is the modified interaction strength. In the present work, we consider condensate consisting of ^{87}Rb atoms in $F = 1$, $m_F = 1$ state with s-wave scattering length equal to $99a_0$ [16]. We have neglected a constant term corresponding to energy along axial direction as it only shifts the energies and chemical potentials by a constant without affecting the dynamics. This equation can be solved numerically by using Crank-Nicholson method [17].

A. Generation of vortex-dipole pairs

There are several theoretical proposals to generate vortices in non-rotating traps. These include stirring of the condensate using blue-detuned laser or several laser beams [3, 14], adiabatic passage [18], Raman transitions in bicondensate systems [19], laser beam vortex guiding [20], laser beam diffraction on a helical light grating [21], and phase imprinting [22]. Among these methods, the easiest one to nucleate vortex dipoles is by stirring a BEC with a blue-detuned laser beam. When the velocity of the laser beam exceeds a critical velocity, vortex-antivortex pairs are released from the localized dip in the number density created due to the laser beam. These vortex dipoles then move through the BEC and exhibit various interesting dynamics [4, 14, 23]. The critical velocity depends on the number density, width and intensity of the laser beam, and the frequency of the trapping potential. This nucleation process exhibits a high degree of coherence and stability, allowing us to map out the annihilation of the dipoles. In an axis symmetric trap, a vortex dipole is a metastable state of superfluid flow with long lifetime.

B. Trajectory of a vortex dipole

The motion of a vortex dipole in a trapped BEC may be understood in terms of two contributions to the velocity of each vortex in the dipole. First, the precession due to the inhomogeneity of the condensate and secondly, the velocity induced by the other vortex. In our case, we have considered highly oblate BEC with a few well separated vortex dipoles, hence the contribution to velocity field due to the other vortex dipoles can be neglected. Moreover, as the obstacle is moved along x-axis, it leads to creation of the vortex dipoles located symmetrically about this axis. The velocity of the each vortex in the dipole is then given by

$$\mathbf{v} = \omega_p\hat{\mathbf{k}} \times \mathbf{r} + \frac{1}{2y}\hat{\mathbf{i}}, \tag{7}$$

where ω_p is the precession frequency, $\hat{\mathbf{k}}$ is the direction of circulation at the location of vortex, and $2y$ is the separation between vortex and antivortex. This equation can be reduced to two equations in xy-plane as

$$\frac{dx}{dt} = -\omega_p y + \frac{1}{2y}, \tag{8}$$

$$\frac{dy}{dt} = \omega_p x. \tag{9}$$

These two equations govern the motion of a vortex dipole. The solutions of these equations with different initial conditions are shown in Fig. 1. From the Fig. 1, one can observe that the vortex dipole come closer only along the x-axis of the BEC. They can even be closer than the coherence length. For this, the vortex needs to be created close to the obstacle. Hence, the annihilation will occur only along the diameter of BEC.

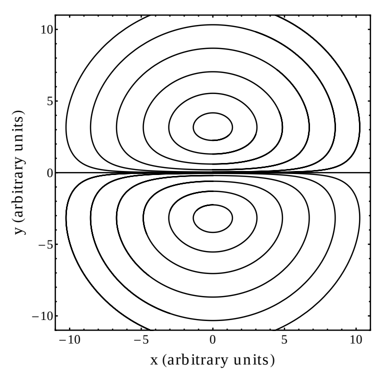

FIG. 1. The trajectories of the vortex dipole in oblate BEC calculated numerically from the equation of motion Eq. (8,9). The trajectories depend on the initial conditions.

III. VORTEX DIPOLE ANNIHILATION

To analyse the vortex dipole annihilation, we consider a model system where the vortex and antivortex are

static. However, we vary the distance of separation and examine the energy of the total system.

The vortex and anti-vortex annihilation occurs when the separation is less than ξ. A simplistic model of a vortex dipoles in the BEC of trapped dilute atomic gases is the superposition of harmonic oscillator eigenstates. The minimalist wave function which supports a vortex and antivortex at cordinates $(-a/c, -\sqrt{b/d})$ and $(-a/c, \sqrt{b/d})$ is

$$\psi(x,y) = \left(ia - b + ixc + dy^2\right) e^{-(x^2+y^2)/f}, \tag{10}$$

where a, b, c, d, and f are positive variational parameters. The wave function is a superposition of the scaled ground state and the first and the second excited states of harmonic oscillator along the x and y-axes, respectively. The wave function is ideal for weakly interacting condensates, however, the qualitative descriptions remain unaltered for strongly interacting condensates. The normalization condition, considering correction for the excited states being negligible, is $a^2 + b^2 = 2/(f\pi)$. This is a constraint equation.

With a slight modification, the trajectory of the vortex dipole can be represented in terms of the time-dependent parameters. For example, the wave function when the vortex dipole is moving along x-axis

$$\psi(x,y,t) = e^{-i\mu t}\left[-b(t) + ic(x-vt) + dy^2\right] e^{-(x^2+y^2)/f}, \tag{11}$$

where v is the velocity with which the vortex dipole moves along the x-axis, and μ is the chemical potential of the system.

A. Diametric vortex dipole

Consider that the vortex and antivortex are located on the diameter of the condensate. Without loss of generality, we consider the diameter as coinciding with the y-axis, which is equivalent to $a = 0$ in Eq. 10. Such an assumption does not modify the qualitative descriptions, but expressions are far less complicated. The wave function is then

$$\psi(x,y,t) = e^{-i\mu t}\left[-b(t) + icx + dy^2\right] e^{-(x^2+y^2)/f}. \tag{12}$$

The nontrivial phase of the wave function θ is discontinuous along $x = 0$ line for $-\sqrt{b/d} \leqslant y \leqslant \sqrt{b/d}$. Across the discontinuity, there is a phase change from $-\pi$ to π as we traverse along x-axis from 0^- to 0^+. To assign phase and elucidate the nature of the phase discontinuity, consider $y = \delta$, a line parallel to x-axis, where $\delta < \sqrt{b/d}$ is a very small positive constant. Along the line $y = \delta$, $(dy^2 - b(t)) < 0$ and at $x \gg 0$, $cx/(dy^2 - b(t)) \to -\infty$ and θ is $\approx \pi/2$. When we decrease x, θ increases and it is $\approx \pi$ when $x \to 0^+$. On the other side of the y-axis, at $x \ll 0$, $cx/(dy^2 - b(t)) \to \infty$ and θ is $\approx -\pi/2$. However, on increasing x the phase θ tends to $-\pi$. So, there is a discontinuity across the y-axis. This is the typical phase pattern associated with vortex dipoles. For the present case, the ground state wave function is

$$\psi_{\rm g}(x,y,t) = -e^{-i\mu t} b(t) e^{-(x^2+y^2)/f}, \tag{13}$$

and from the normalization condition $\int_{-\infty}^{\infty}\int_{-\infty}^{\infty} |\psi_{\rm g}|^2 dxdy = 1$, we get the constraint equation

$$b^2 = \frac{2}{f\pi}. \tag{14}$$

For general considerations, rewrite the additional term as

$$\delta\psi(x,y,t) = e^{-i\mu t}\left(icxe^{-i\omega t} + dy^2 e^{i\omega t}\right) e^{-(x^2+y^2)/f}. \tag{15}$$

So that the total wave function $\psi = \psi_{\rm g} + \delta\psi$, where $\delta\psi$ represents an elementary excitation of the condensate. From the Bogoliubov theory, it satisfies the normalization condition

$$\int_{-\infty}^{\infty}\int_{-\infty}^{\infty} \left(c^2x^2 - d^2y^4\right) e^{-2(x^2+y^2)/f} dxdy = 1, \tag{16}$$

which after evaluation is

$$\frac{\pi f^2}{4}(2c^2 - 3d^2 f) = 1. \tag{17}$$

The limits, in reality, must be the physical size of the condensate clouds. However, due to the exponential decay and relatively large extent of the condensate clouds there is little difference in the results. The Eq. (17), like Eq. (14), is an additional constraint equation to the wave function. We can calculate the total energy of the system, without the obstacle potential, as

$$E_{\rm vd} = \int_{-\infty}^{\infty}\int_{\infty}^{\infty} \left[\frac{1}{2}|\nabla_\perp\psi(x,y)|^2 + \frac{x^2+y^2}{2}|\psi(x,y)|^2 + u|\psi(x,y)|^4\right] dxdy. \tag{18}$$

This is the energy of condensate with a vortex dipole with the assumption that it is a weakly interacting system. Energy without the vortex may be calculated trivially [10]. In general, the energy added to the system due to the vortex dipole is not large compared to the total and for obvious reason, the angular momentum of the condensate is still zero.

B. Grey soliton

A slight modification to the wave function can describe a solitonic solution along y-axis. The form of the modifed wave function is

$$\psi(x,y) = \left[b(t) + icx + dy^2\right] e^{-(x^2+y^2)/f}, \tag{19}$$

where except for the change in the sign of b, all the terms remain unaltered as in Eq. (10). It is a *grey* soliton as

the density $n \propto (b + dy^2)^2 + (a + cx)^2$ has a dip but is different from zero.

Like in vortex dipole, we examine the nature of the phase around the points $(0, -\sqrt{b/d})$ and $(0, \sqrt{b/d})$. The nontrivial phase of the wave function θ has no discontinuities. Consider again the line $y = \delta \ll \sqrt{b/d}$, which is parallel to x-axis. Along the line $(dy^2 + b(t)) > 0$ at all values of x and $-\pi/2 \leqslant \theta \leqslant \pi/2$. In the $x \gg 0$ domain, $cx/(dy^2 + b(t)) \to \infty$ and $\theta \approx \pi/2$. When we decrease x, θ decreases and it is ≈ 0 when $x \to 0^+$. On the other side of the y-axis, at $x \ll 0$ the phase $\theta \approx -\pi/2$. However, on decreasing x the phase θ tends to 0. So, the phase varies smoothly from $-\pi/2$ to $\pi/2$ along the normal to the line which connects $(0, -\sqrt{b/d})$ and $(0, \sqrt{b/d})$.

Using the wave function in Eq. (19), we can then evaluate the total energy of the system $E_{\rm gs}$. We define the energy difference between the two states of the condensates as

$$\Delta E = E_{\rm vd} - E_{\rm gs}, \tag{20}$$

which after evaluation is

$$\Delta E = \frac{bdf^2\pi}{256}\left[64b^2u + 15d^2f^2u + 8f(8 + c^2u)\right]. \tag{21}$$

The most general solution is when all the constants are positive, then $\Delta E > 0$ and the grey soliton is lower in energy. This shows that when the vortex-antivortex collides, it is energetically favourable for them to decay into grey soliton. As discussed in the results section, this is confirmed in the numerical calculations.

The analysis so far is for an ideal system at zero temperature, where we have neglected the thermal fluctuations and perturbations from imperfections. In addition, there is dissipation from three body collision losses in the condensates of dilute atomic gases.

IV. NUMERICAL RESULTS

The specific paremeters we consider for the numerical studies are: the species is chosen as ^{87}Rb with $N = 2 \times 10^6$ atoms. The trapping potential and obstacle laser potential parameters are same as those considered in Ref. [3], i.e., $\omega/(2\pi) = 8$ Hz, $\beta = 11.25$, $V_0(0) = 93.0\ \hbar\omega$ and $w_0 = 10\ \mu$m. The obstacle potential $V_{\rm obs}$ is initially located at $-12.5\ a_{\rm osc}$. To nucleate vortices, we move the obstacle along the x direction at a constant velocity with decreasing intensity until $V_{\rm obs}$ vanishes at $5.18\ a_{\rm osc}$.

A. Vortex dipole nucleation

We study the nucleation of vortices by $V_{\rm obs}$ with the translation speed v ranging from 80 μm/s to 200 μm/s. Vortices are not nucleated when the speed is 80 μm/s. However, a vortex-antivortex or a vortex dipole is nucleated when the speed is in the range 90 μm/s $< v <$ 140 μm/s. Increasing the speed of obstacle generates two pairs in 140 μm/s $\leqslant v <$ 160 μm/s and more than two when $v \geqslant 160$ μm/s. In other words, the number of vortex dipoles created can be controlled with the speed of the obstacle. Creation of vortex dipoles above a critical speed v_c is natural as the vortex nucleation must satisfy the Landau criterion [24]. The density and phase of the condensate after the nucleation of vortex dipole for $v = 160$ μm/s is shown in Fig. 3. The figure clearly shows nucleation dynamics of the vortex dipoles.

Through a series of calculations, we determine $v_c \approx 90$ μm/s. This is, however, less than the acoustic velocity of the medium s, which depends on the local condensate density $s = \sqrt{nU/m}$. This also explains the reason for the predominant vortex dipole nucleation around the edge of the condensate where the density is lower and the acoustic speed is accordingly lower.

B. Vortex dipole annihilation

It is observed that the vortex dipole annihilation is critically dependent on the initial conditions of the nucleation. For this reason, the annihilation events are observed only for specific range of v. As an example, the annihilation event when v is 120 μm/s is shown in Fig. 2. In Fig. 2, we can notice the density minima arising from the annihilation and propagating away from the $V_{\rm obs}$.

One observation, which is common to all the vortex dipoles getting annihilated is the nature of their trajectory. All of them traverse through $V_{\rm obs}$, whereas the ones which do not get annihilated avoid $V_{\rm obs}$. This is again

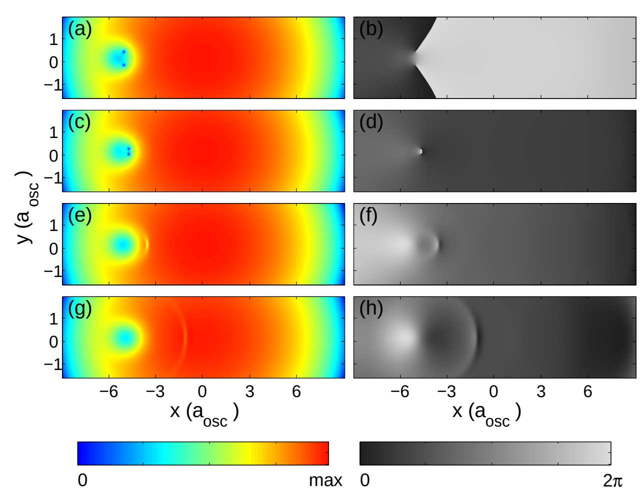

FIG. 2. A vortex dipole is nucleated when the obstacle potential traverses the condensate at a speed of 120 μm/s. The vortex dipole, however, passes through and overtakes the obstacle. Later, as seen in (e), the vortex dipole annihilates and generates a grey soliton. The figures in the left panel show the density distribution and those on the right show the phase pattern of the condensate.

related to the initial conditions. The vortex dipoles are generally nucleated at the aft region of the V_{obs} where there is a trailling superflow. When nucleated very close to each other and with high velocity, the mutual force further increases the velocity of the vortex dipoles. At the same time, it decreases the distance separating vortex and antivortex. So, the kinetic energy is high enough to surpass V_{obs}. Later, at some point vortex and antivortex separation is less than ξ, and they annihilate.

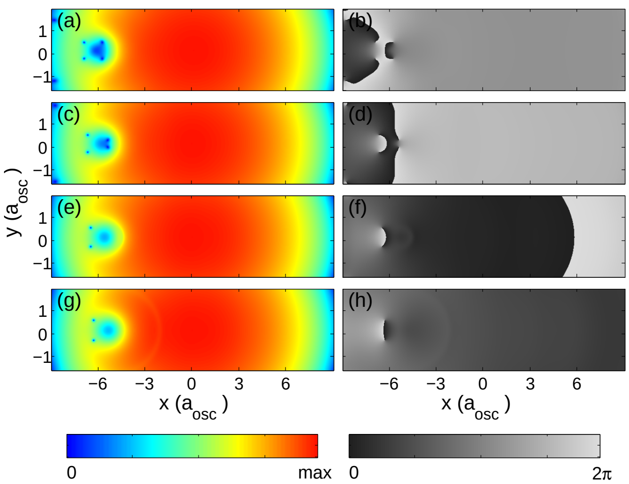

FIG. 3. A vortex dipole is nucleated as the obstacle potential traverses the BEC with a speed of 160 μm/s. The figures in the left panel shows the density with time, where time progresses from top to bottom. Figures on the right panel show the phase pattern of the condensate.

A reliable and qualitative way to describe occurrence of annihilation could be achieved by observing the density at the cores of vortex and antivortex which form the dipole. For the vortex, the matter density at the core when v is 120 μm/s is shown in Fig 4. In the plot, at Time $\approx$ 900 (arbitrary units), the core density starts increasing. This is because the core starts to fill in with the atoms from around the vortex after the annihilation.

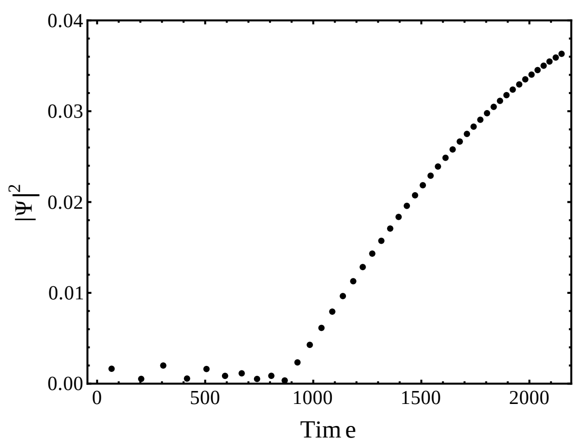

FIG. 4. Density variation at the core of the vortex with time (in scaled unit). After the vortex dipole annihilation, density increases till it reaches the bulk value. The values correspond to 120 μm/s obstacle speed.

As discussed in Section. III B, annihilation can occur only when it is energetically favorable. In other words, the state with the grey soliton must have lower energy than the vortex dipole. This is clearly seen in the change of total energy of the system, which is shown in Fig. 5. After the annihilation, the energy of the system decreases and continues to do so at a steady rate. Although not shown in the plot, before the annihilation the energy is on an average constant. The energy change, can thus be considered as a very good signature of the annihilation of vortex dipoles.

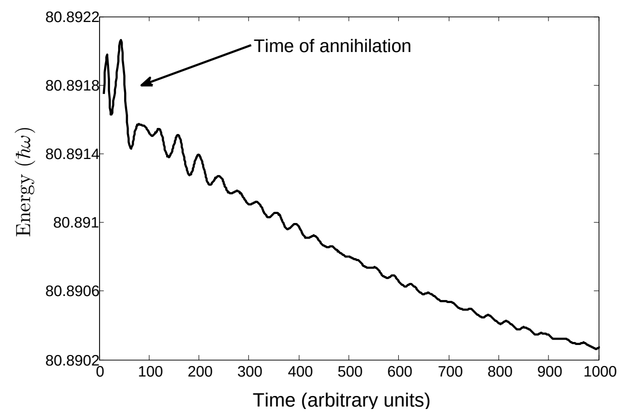

FIG. 5. Variation in the energy of the system with time (in scaled units). There is a decrease in energy after the vortex dipole annihilation, and the plot is based on the results of calculations in which a vortex dipole is imprinted at ($-2.0\ a_{\text{osc}}$, $\pm 0.1\ a_{\text{osc}}$). It is then allowed to annihilate and evolve in time.

It is to be mentioned that for the parameters considered in the present work, the speed of sound is 2190 μm/s, which is similar to the speed observed by Neely et. al. [3]. The coherence length of the system is $\sim 0.25\ \mu$m and the minimum distance between the vortex dipole pair is $\sim 0.3\ \mu$m. The position of annihilation determined from the equation of motion (Eq. 8-9) matches with those obtained from the simulation.

C. Effect of noise and dissipation

In the numerical studies, the annihilation events are not rare. But, this is in contradiction with the experimental results of Neely and collaborators [3], they observed no signatures of annihilation events. One possible reason is that our numerical calculations are too ideal, and one immediate remedy is to include fluctuations. For this we introduce white noise during the real time evolution. One immediate outcome is, the symmetry in the

trajectory of the vortex and antivortex is lost. The superflow around the vortex is no longer a mirror reflection of the antivortex, which was nearly the case without the white noise. The deviations are shown for an example case in the Fig. 6. The change in path leads to the suppression of annihilation of vortex dipoles.

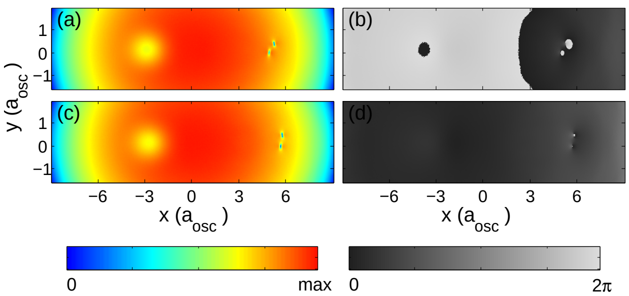

FIG. 6. The trajectory of a vortex dipole in the presence of white noise. There is a lack of symmetry in the trajectory of the vortex and antivortex. This reduces the possibility of an annihilation event significantly. The figures in the left (right) panel show the density (phase) of the condensate and time increases from top to bottom figures of each panel. The speed of the obstacle is 180 μm/s, and the white noise is at the level of 0.01%.

The other important effect is the loss of atoms from the trap. We have examined the effect of loss terms, which arise from inelastic collisions in the condensate. There are two types of inelastic collisions that lead to the loss of atoms from the trap: two body inelastic collision loss and the three body loss. To model the effect of loss of atoms from the trap, we add the loss terms

$$\frac{-i\hbar}{2}\left(K_2|\Psi(\mathbf{r},t)|^2 + K_3|\Psi(\mathbf{r},t)|^4\right), \tag{22}$$

to the Hamiltonian $\mathcal{H}$. Based on the previous work [25] for ^{87}Rb, the inelastic two-body loss rate coefficient $K_2 = 4.5 \times 10^{-17}$ cm^3 s^{-1}, and inelastic three-body loss rate coefficient $K_3 = 3.8 \times 10^{-29}$ cm^6 s^{-1}. With trap loss, the annihilation events continue to occur. However, during the destructive time of flight observations in the experiments, the decreased atom numbers may lower the contrast and reduce the possibility of observing an annihilation event.

V. CONCLUSIONS

When an obstacle moves through a condensates above a critical speed, it nucleates vortex dipoles and the number of dipoles seeded depends on the obstacle velocity. Depending on the initial condition of nucleation, vortex and antivortex annihilation events occur under ideal conditions: at zero temperature, no loss, and without noise. However, the noise destroys the superflow reflection symmetry around the vortex and antivortex. This reduces the possibility of annihilation events and may explain the lack of annihilation events in experimental observation in Ref. [3].

ACKNOWLEDGMENTS

The numerical calculations reported in this paper have been performed on 3 TeraFlop high-performance cluster (HPC) at Physical Research Laboratory (PRL), Ahmedabad.

[1] J. R. Anglin and W. Ketterle, Nature **416**, 211 (2002).
[2] M. R. Matthews, B. P. Anderson, P. C. Haljan, D. S. Hall, C. E. Wieman, and E. A. Cornell, Phys. Rev. Lett. **83**, 2498 (1999).
[3] T. W. Neely, E. C. Samson, A. S. Bradley, M. J. Davis, and B. P. Anderson, Phys. Rev. Lett. **104**, 160401 (2010).
[4] D. V. Freilich, D. M. Bianchi, A. M. Kaufman, T. K. Langin, and D. S. Hall, Science **329**, 1182 (2010).
[5] J. Brand and W. P. Reinhardt, Phys. Rev. A **65**, 043612 (2002).
[6] S. Middelkamp, P. J. Torres, P. G. Kevrekidis, D. J. Frantzeskakis, R. Carretero-Gonzlez, P. Schmelcher, D. V. Freilich, and D. S. Hall, Phys. Rev. A **84**, 011605(R) (2011).
[7] T. K. T. Aioi, T. Kadokura and H. Saito, Phys. Rev. X **1**, 021003 (2011).
[8] Y. Couder and C. Basdevant, Journal of Fluid Mechanics **173**, 225 (1986).
[9] D. G. Grier, Nature **424**, 810 (2003).
[10] C. Pethick and H. Smith, *Bose-Einstein Condensation in Dilute Gases* (Cambridge University Press, 2002).
[11] A. L. Fetter, Rev. Mod. Phys. **81**, 647 (2009).
[12] E. B. Sonin, Rev. Mod. Phys. **59**, 87 (1987).
[13] S. Alekseenko, P. Kuibin, and V. Okulov, *Theory of Concentrated Vortices* (Cambridge University Press, 2002).
[14] B. Jackson, J. F. McCann, and C. S. Adams, Phys. Rev. A **61**, 013604 (1999).
[15] W. Li, M. Haque, and S. Komineas, Phys. Rev. A **77**, 053610 (2008).
[16] E. G. M. van Kempen, S. J. J. M. F. Kokkelmans, D. J. Heinzen, and B. J. Verhaar, Phys. Rev. Lett. **88**, 093201 (2002).
[17] P. Muruganandam and S. Adhikari, Computer Physics Communications **180**, 1888 (2009).
[18] R. Dum, J. I. Cirac, M. Lewenstein, and P. Zoller, Phys. Rev. Lett. **80**, 2972 (1998).
[19] K. P. Marzlin, W. Zhang, and E. M. Wright, Phys. Rev. Lett. **79**, 4728 (1997).
[20] K. Staliunas, Applied Physics B: Lasers and Optics **71**, 555 (2000).

[21] C. Weiss, M. Vaupel, K. Staliunas, G. Slekys, and V. Taranenko, Applied Physics B: Lasers and Optics **68**, 151 (1999).

[22] G. Andrelczyk, M. Brewczyk, L. Dobrek, M. Gajda, and M. Lewenstein, Phys. Rev. A **64**, 043601 (2001).

[23] P. Kuopanportti, J. A. M. Huhtamäki, and M. Möttönen, Phys. Rev. A **83**, 011603 (2011).

[24] E. M. Lifshitz and L. P. Pitaevskii, *Statistical Physics, Part 2* (Pergamon Press, Oxford, 1980).

[25] J. P. Burke, J. L. Bohn, B. D. Esry, and C. H. Greene, Phys. Rev. Lett. **80**, 2097 (1998).